Environmental Science & Technology

Article

pubs.acs.org/est

Effect of Pellet Boiler Exhaust on Secondary Organic Aerosol Formation from α-Pinene

Eetu Kari,[†] Liqing Hao,[†] Pasi Yli-Pirilä,[†] Ari Leskinen,[†,§] Miika Kortelainen,[‡] Julija Grigonyte,[‡] Douglas R. Worsnop,[†,¶,∥] Jorma Jokiniemi,[‡] Olli Sippula,[‡] Celia L. Faiola,[†] and Annele Virtanen*[,†]

[†]Department of Applied Physics, University of Eastern Finland, P.O. Box 1626, 70211 Kuopio, Finland

[§]Finnish Meteorological Institute, Kuopio Unit, P.O. Box 1627, 70211 Kuopio, Finland

[‡]Department of Environmental and Biological Sciences, University of Eastern Finland, P.O. Box 1627, 70211 Kuopio, Finland

[¶]Aerodyne Research, Inc., Billerica, Massachusetts 08121-3976, United States

[∥]Department of Physics, University of Helsinki, P.O. Box 64, 00014 Helsinki, Finland

Supporting Information

ABSTRACT: Interactions between anthropogenic and biogenic emissions, and implications for aerosol production, have raised particular scientific interest. Despite active research in this area, real anthropogenic emission sources have not been exploited for anthropogenic-biogenic interaction studies until now. This work examines these interactions using α-pinene and pellet boiler emissions as a model test system. The impact of pellet boiler emissions on secondary organic aerosol (SOA) formation from α-pinene photo-oxidation was studied under atmospherically relevant conditions in an environmental chamber. The aim of this study was to identify which of the major pellet exhaust components (including high nitrogen oxide (NO_x), primary particles, or a combination of the two) affected SOA formation from α-pinene. Results demonstrated that high NO_x concentrations emitted by the pellet boiler reduced SOA yields from α-pinene, whereas the chemical properties of the primary particles emitted by the pellet boiler had no effect on observed SOA yields. The maximum SOA yield of α-pinene in the presence of pellet boiler exhaust (under high-NO_x conditions) was 18.7% and in the absence of pellet boiler exhaust (under low-NO_x conditions) was 34.1%. The reduced SOA yield under high-NO_x conditions was caused by changes in gas-phase chemistry that led to the formation of organonitrate compounds.

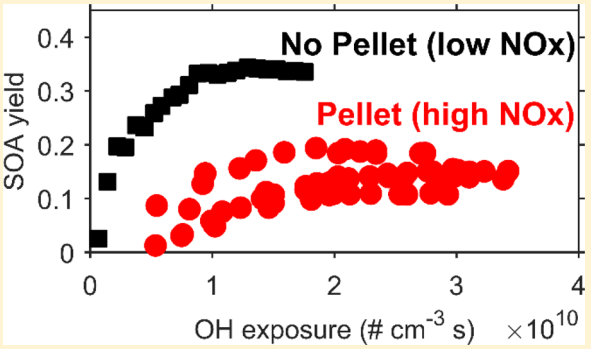

1. INTRODUCTION

Volatile organic compounds (VOCs) are emitted into the atmosphere from biogenic and anthropogenic sources. Once they are in the atmosphere, VOCs undergo a number of chemical and physical processes that result in the formation of secondary pollutants, such as ozone and secondary organic aerosols (SOA).[1,2] SOA, a major component of atmospheric aerosols, impacts climate by influencing the size distribution, chemical composition, and radiative and cloud formation properties of the atmospheric particle population.[3,4] Consequently, accurate representations of SOA production are crucial for reducing uncertainties in climate change estimates. However, models continue to underestimate SOA production when compared to field measurements.[4] The largest source of atmospheric VOCs that lead to SOA formation is emissions from vegetation, called biogenic volatile organic compounds (BVOCs). Annual BVOC emissions are estimated to be 825−1150 TgC yr^{-1}.[5,6] In contrast, anthropogenic VOC emissions account for ∼140 TgC yr^{-1} of atmospheric VOCs.[7] However, anthropogenic emissions can dominate VOCs in urban areas[8−10] and are also a major source of primary particulate pollution with a global estimate of 65 Tg yr^{-1}.[11]

In the natural atmosphere, anthropogenic and biogenic sources of pollutants do not exist in isolation, and the potential interaction between the two pollutant sources has raised particular scientific interest. One objective of previous studies on this topic has been to explore the impact of anthropogenic emissions on biogenic SOA formation and its climate-relevant characteristics.[12−17] BVOCs and anthropogenic emissions can interact via several mechanisms that were reviewed by Hoyle et al.[18] Some of these mechanisms include interactions between BVOCs and primary particles emitted by anthropogenic sources. For example, emissions of anthropogenic primary organic aerosol (POA) can increase organic aerosol mass loadings and enhance partitioning of BVOC oxidation products to the particle phase if the anthropogenic POA forms a miscible

Received: September 28, 2016
Revised: December 13, 2016
Accepted: December 23, 2016
Published: December 23, 2016

DOI: 10.1021/acs.est.6b04919
Environ. Sci. Technol. 2017, 51, 1423−1432

Table 1. Initial Experimental Conditions and the Results

experiment	experiment ID	initial mass loading ($\mu g\ m^{-3}$)[a]	dilution factor[c]	total OA ($\mu g\ m^{-3}$)[d,g]	THC in raw exhaust (ppm)	initial α-pinene concn (ppb)[e]	VOC-to-NO_x ratio (ppbC/ppb)	NO_x concn (ppb)	maximum OH exposure (cm^{-3} s)	yield[f]
Pellet	Pellet	95 ± 4.5	228	8.9 ± 0.10	36.5		10	455	3.7E10	
Pellet+α-pin	LowP+α	25 ± 4.0	241	12.7 ± 0.17	25.7	17.0 ± 0.12	6.5	570	2.9E10	0.114 ± 0.0156
Pellet+α-pin	MedP+α1	47 ± 3.0	237	16.7 ± 0.12	23.3	16.2 ± 0.14	4.7	625	3.1E10	0.140 ± 0.0113
Pellet+α-pin	MedP+α2	45 ± 3.5	221	20.4 ± 0.14	22	17.9 ± 0.18	6.0	625	3.3E10	0.146 ± 0.0471
Pellet+α-pin	MedP+α3	82 ± 3.0	224	19.9 ± 0.18	14.9	15.5 ± 0.71	5.9	695		0.146 ± 0.0140
Pellet+α-pin	HighP+α	93 ± 4.0	209	25.6 ± 0.25	19.5	16.0 ± 0.16	7.2	615	2.7E10	0.187 ± 0.0142
AS+α-pin	LowAS+α	17 ± 3.0		12.7 ± 0.10		19.4 ± 0.18	4.6	685	3.8E10	0.120 ± 0.0124
AS+α-pin	MedAS+α	68 ± 4.5		10.2 ± 0.20		14.6 ± 0.09	5.3	565	3.7E10	0.130 ± 0.0210
AS+α-pin	HighAS+α	149 ± 5.5		13.5 ± 0.21		13.8 ± 0.09	5.3	695	2.9E10	0.179 ± 0.0170
AS+α-pin	LowNO_x	23 ± 1.9[b]		26.4 ± 0.42		20.3 ± 0.14			2.3E10	0.341 ± 0.0187

[a]Initial mass loadings were determined by TEOM; stated uncertainties (1σ) are estimated from scatter in mass concentration measurements. [b]Initial mass loading of the Low-NO_x experiment was determined by SMPS; stated uncertainty (1σ) is estimated from scatter in mass concentration measurements. [c]Dilution ratios were determined from the dilution of CO_2 concentration that was measured from raw pellet boiler emission by FTIR and from the chamber by CO_2 analyzer. [d]Stated uncertainties (1σ) are estimated from scatter in organic aerosol mass concentration measured by SP-AMS. [e]Stated uncertainties (1σ) are estimated from scatter in PTR-MS measurements or from GC-MS measurements for the MedP+α3 experiment. [f]Stated uncertainties are estimated from uncertainties in SP-AMS and PTR-MS measurements using square root of sum of squares of relative standard deviations (for the MedP+α3 experiment uncertainty is estimated from uncertainties in SP-AMS and GC-MS measurements). [g]For pellet boiler experiments Total OA = POA+SOA.

phase with BVOC oxidation products.[19−21] Additionally, anthropogenic emissions can enhance acidic seed material in the atmosphere via the production of sulfuric acid and nitric acid.[22] Acidic particles catalyze particle-phase reactions like hydration, hemiacetal and acetal formation, aldol condensation, oligomerization, and polymerization.[22−24] These reactions result in the formation of low-volatility products that enhance gas-particle partitioning and SOA formation. Anthropogenic emissions can also interact with BVOCs via mechanisms involving gas-phase chemistry. For example, increased concentrations of nitrogen oxides (NO_x), sulfur dioxide (SO_2), and/or aromatic VOCs can influence SOA formation from BVOCs. Higher concentrations of NO_x change gas-phase reaction pathways because NO starts to compete with HO_2 and RO_2 for alkyl peroxy radicals formed during the first stages of VOC oxidation.[25,26] The high-NO_x oxidation pathway leads to different functional groups in the oxidation products and can also influence fragmentation of compounds during oxidation. Alterations to the functionalization and fragmentation of BVOC oxidation products can increase or decrease SOA formation depending on the specific BVOC precursors. For example, elevated NO_x increases SOA yields of β-caryophyllene[27] but decreases SOA yields of α-pinene[25] because of their different structures. Higher levels of SO_2 enhance new particle formation and growth[28] and increase particle acidity via the production of H_2SO_4. This increases the acidity of particles in the atmosphere and promotes acid-catalyzed reactions that were described previously.

Anthropogenic-biogenic interactions are often studied using mixtures of standard compounds that are meant to represent typical compounds from each source.[18] There have been no controlled laboratory studies investigating the topic using real emission sources, which are more chemically diverse and better represent the complex chemical composition in the atmosphere. The primary aim of this study was to investigate anthropogenic-biogenic interactions using pellet boiler exhaust as a real anthropogenic emission source. Pellet boilers are commonly used in homes for heating purposes due to their automated operation, high energy density of pellets, high efficiency, and lower emissions compared to old wood log appliances.[29−31] In addition, there is also growing interest to utilize wood pellets in larger scale heat and power plant boilers to increase the production of renewable energy. Pellet boilers emit aliphatic, aromatic, and oxygenated VOCs and also inorganic species such as NO_x, ash, and black carbon (BC).[32−34] In this study, we investigated the impact of pellet boiler emissions on SOA formation from α-pinene photooxidation. The aim of the study was to determine whether high NO_x concentrations or the primary particles emitted by the pellet boiler, or a combination of these two mechanisms, affected SOA formation from α-pinene. The experiments were conducted in a 29 m^3 environmental chamber under atmospherically relevant VOC-to-NO_x ratios. To our knowledge this is the first study investigating anthropogenic-biogenic interactions using a real anthropogenic emission source rather than pure compounds to represent an anthropogenic source. This approach will provide a more realistic picture of the possible mechanisms by which anthropogenic emissions can interact with BVOCs in the atmosphere.

2. EXPERIMENTAL SECTION

2.1. Experimental Setup. The schematic of the experimental setup is shown in Figure S1. A detailed characterization of the chamber facility was reported by Leskinen et al.[35] Briefly, the experiments were carried out in a 29 m^3 fluorinated ethylene propylene resin (Teflon FEP) environmental chamber located at the University of Eastern Finland in Kuopio, Finland. The chamber was a collapsible bag equipped with 40 W blacklight (BL) lamps having a spectrum centered at 354 nm (Sylvania F40W/350 BL) located on two opposite sides of the chamber. The chamber was placed in a thermally insulated enclosure, and the temperature inside the enclosure was

DOI: 10.1021/acs.est.6b04919
Environ. Sci. Technol. 2017, 51, 1423−1432

controlled by a thermostated air conditioner (Argo AW 764 CL3). The inner walls of the temperature-controlled enclosure around the chamber were covered by reflective materials for enhancing and evenly distributing the UV radiation.

Table S1 summarizes the instrumentation used in this study, and the detailed information can be found in the Supporting Information (SI). Both gas- and particle-phase measurements were conducted. Gas-phase VOC monitoring was performed with a high sensitivity proton-transfer-reaction time-of-flight mass spectrometer (hereafter referred to as the PTR-MS), and specific trace gas measurements included the following gases: CO_2, CO, NO_x ($NO+NO_2$), and O_3. Some of the most common volatile organic compounds for wood combustion exhaust, including 28 hydrocarbons and oxygenated hydrocarbon species (Table S2), were also measured from the raw exhaust by Fourier Transform Infrared Spectroscopy (FTIR). In addition, two cartridge samples (Tenax TA/Carbograph 5TD adsorbent material, MARKES international, United Kingdom) were collected during each experiment and were analyzed off-line using a thermal desorption-gas chromatograph−mass spectrometer (TD-GC-MS). The chemical composition of the particle-phase was monitored with an Aerodyne, Inc. soot particle-aerosol mass spectrometer (SP-AMS). Particle mass and number concentrations and size distributions were measured using a tapered element oscillating microbalance (TEOM) and scanning mobility particle sizer (SMPS).

2.2. Experimental Procedure. Prior to each experiment the chamber was cleaned (details in the SI). Before starting the experiments, relative humidity of the chamber was adjusted to ∼50%, and the temperature was held constant at ∼20 °C with a thermostated air conditioner. A commercially available pellet boiler with a nominal heat output of 25 kW was used for these experiments.[36] Bark-free softwood pellets were used as the fuel. The detailed information about the pellet boiler exhaust feeding procedure can be found from the SI.

After the diluted primary pellet emissions were fed into the chamber, O_3 was added in the amount required to convert all the NO emitted from the pellet boiler to NO_2. NO must be converted to NO_2 to prevent the suppression of photochemistry and subsequent SOA formation.[37,38] After O_3 addition, ∼1 μL of 9-fold deuterated butanol (1-butan,d_9-ol, hereafter referred to as butanol-d9, Sigma-Aldrich, 98%) and ∼3 μL (17 ppbv) of α-pinene (Sigma-Aldrich, ≥99%) were injected into the chamber. Butanol-d9 was used to quantify the OH exposure during the experiments (details from the SI).[39] OH radicals were generated from nitrous acid (HONO). HONO was prepared by dropwise addition of 1% $NaNO_2$ into 10% H_2SO_4 in a glass bottle. The bottle was attached to the inlet line and purged with air to transport HONO into the chamber. To prevent immediate termination and destruction of OH radicals, the VOC-to-NO_x ratio was adjusted to atmospherically relevant levels (Table 1) using propene from a standard gas cylinder (10000 ppm in N_2, AGA, Finland) following previously established methods.[40] Propene chemistry allows recycling of OH radicals, but its oxidation products do not contribute to SOA formation.[19,37] After all gases and exhaust were introduced, the chamber was closed, and gases were allowed to stabilize for 15 min. After gas concentrations stabilized, BL-lamps were switched on to initiate photochemistry (designated the experiment start time), and the experiment was run for another 4 h.

Results from this study represent an upper-bound estimate of potential pellet emissions and biogenic-anthropogenic interactions. The pellet boiler was operated under nonoptimal combustion conditions which occur for example in partial boiler load situations,[36] and when the users operate their boilers with nonoptimally adjusted settings—scenarios that are arguably not uncommon. The particle mass concentration of pellet boiler exhaust fed into the chamber was estimated from SMPS data. The initial mass loading of primary particles in the chamber was systematically varied between 25 and 95 μg m^{-3} from experiment to experiment, but other conditions were kept unchanged, including α-pinene concentration, VOC-to-NO_x ratio, and OH exposure (Table 1). For some experiments, pellet boiler exhaust was not used, and the initial particle mass loading was replaced with ammonium sulfate (AS) seed particles (Sigma-Aldrich, 99%). AS seed particles were used for comparison to determine if the chemical characteristics of the primary particles emitted by the pellet boiler affected SOA formation from α-pinene. AS particles were generated by a nebulizer (Topas ATM 226, Germany) and were introduced into the environmental chamber through a silica dryer with similar initial mass loadings that were used with pellet boiler exhaust experiments (refer to Table 1). In experiments with AS particles, all experimental conditions like VOC-to-NO_x ratio, NO_x concentration, and OH exposure were comparable to the pellet boiler exhaust experiments (Table 1). In addition to the AS+α-pinene experiments that were conducted under high-NO_x conditions, we also conducted one AS+α-pinene experiment under low-NO_x conditions. The experiment under low-NO_x conditions was done to investigate the effect of high-NO_x concentrations emitted by the pellet boiler on SOA formation from α-pinene. This experiment was conducted in a separate 10 m^3 Teflon chamber under similar conditions as the high-NO_x experiments (Table 1). A detailed description of the 10 m^3 chamber and experimental procedure for the low-NO_x experiment is included in the SI.

3. RESULTS AND DISCUSSION

Results from this investigation shed light on biogenic-anthropogenic interactions in the atmosphere using α-pinene and pellet boiler emissions as a model test system. In this section, we first characterize the primary emissions from the pellet boiler to provide context for the possible interactions that could occur between pellet boiler emissions and α-pinene. Next, we characterize SOA formation from pellet boiler emissions with and without α-pinene. These results demonstrated that the primary source of SOA in these experiments was derived from the oxidation of α-pinene and not from the oxidation of the pellet boiler emissions themselves. Finally, we present the α-pinene SOA mass yields in the presence of pellet boiler emissions (hereafter referred to as "mixed" experiments) and compare them with α-pinene SOA mass yields measured in the absence of an anthropogenic influence (hereafter referred to as "α-pinene only" experiments). From these results, we concluded that pellet boiler emissions reduced SOA mass yields from α-pinene photo-oxidation primarily due to the presence of higher concentrations of gas-phase nitrogen oxides.

3.1. Characterization of Pellet Boiler Primary Emission. The composition of pellet boiler primary emissions is summarized in Figure 1 (Experiment ID = Pellet). The upper panel of Figure 1 shows the primary organic aerosol (POA) composition measured with the AMS during the stable, nonoptimal burning phase. POA composition was dominated

DOI: 10.1021/acs.est.6b04919
Environ. Sci. Technol. 2017, 51, 1423−1432

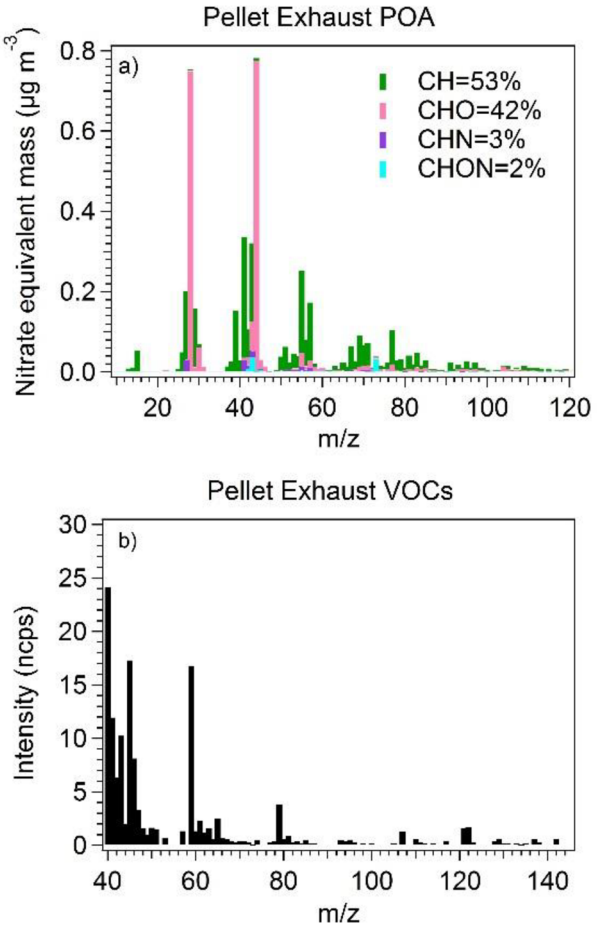

Figure 1. Mass spectra of particle- (upper panel) and gas-phase (lower panel) of primary emission produced by the pellet boiler. The baseline measured through active carbon is subtracted from the gas-phase spectrum, and the water-triplet signal from m/z 55 is removed for clarity.

by hydrocarbons and oxygenated hydrocarbons accounting for 95% of total AMS organic signal. This is consistent with results presented by Heringa et al.;[41] they measured POA composition from pellet burners under poor burning conditions and found that hydrocarbons and oxygenated hydrocarbons accounted for 97% of the total AMS organic signal. A complete mass defect plot of the primary particulate composition is included in the SI to provide additional information on the composition (Figure S2). Of particular interest, the ratio of NO^+-to-NO_2^+ can indicate the source of the nitrate signal. For example, when this ratio is close to 5 it indicates that the NO^+ and NO_2^+ ions are derived from organonitrates.[42,43] The measured NO^+-to-NO_2^+ for pellet primary particulate emissions in this study was 21.8 indicating that the NO^+ and NO_2^+ ions are derived from mineral nitrates.[42] This suggests that this AMS spectra was representative of a combination of POA and ash particulate emissions.

The gas-phase mass spectrum during the stable, nonoptimal burning phase of the pellet boiler is presented in the lower panel of Figure 1. The mass spectrum, measured with PTR-MS, shows that the number of gas-phase compounds emitted by the pellet boiler was low inside the chamber. Furthermore, FTIR measurements show that raw, undiluted pellet boiler exhaust did not contain high concentrations of gas-phase hydrocarbons or oxygenated hydrocarbons. The sum concentration of all analyzed hydrocarbons (THC) varied from 14.9 to 36.5 ppm in raw pellet boiler exhaust (Table 1). This suggests that even under nonoptimal operating conditions, the combustion efficiency of the pellet boiler remained high. The combustion efficiency can be estimated from modified combustion efficiency (MCE = $[CO_2]/([CO]+[CO_2])$). In pellet burner experiments performed by Heringa et al. MCE was 0.999 during stable burning conditions and 0.988 during nonoptimal burning conditions.[41] In our experiments MCE varied from 0.988 to 0.996 demonstrating that the pellet boiler was operated under nonoptimal burning conditions.

The main gas-phase compounds and/or fragments of compounds measured with the PTR-MS in the environmental chamber immediately after the feeding period were C_3H_4 (m/z 41), C_2H_2O (m/z 43), acetaldehyde (m/z 45), acetone (m/z 59), and benzene (m/z 79). All of these VOCs have been detected in pellet boiler exhaust previously.[32−34] However, other studies have also reported pellet boiler emissions of aromatic compounds such as polycyclic aromatic hydrocarbons (PAHs), toluene, and xylene.[32−34] In this study, pellet emissions were substantially diluted to ensure that primary particulate mass loadings were representative of atmospheric conditions in the chamber (see Experimental section 2.2 and Table 1). So while some of those compounds, like toluene, were emitted by the pellet boiler used in this study, their concentrations inside the environmental chamber were not above the detection limit of the PTR-MS.

3.2. Characterization of SOA Production. The pellet boiler emissions did generate a small amount of SOA after oxidation by OH and ozone (Figure 2). These results have not

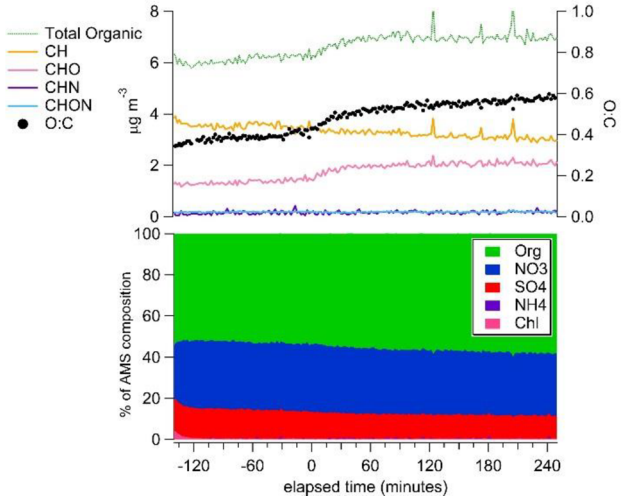

Figure 2. Temporal evolution of OA species (upper panel) and particle-phase species (lower panel) during the Pellet experiment. At time 0 BL-lamps were turned on, and at time 240 the experiment was stopped. The feeding of pellet boiler exhaust is not shown.

been corrected for particle wall-loss because the focus here is to discuss the trends in the organic aerosol species. The lower panel of Figure 2 shows the temporal evolution of the relative aerosol composition throughout the "pellet-only" experiment (Experiment ID: Pellet, Table 1). When photochemistry started, there was a small change in the relative proportion of organics in the particle-phase. These results demonstrate that in the absence of other VOC sources the oxidation of emissions from the pellet boiler operating under nonoptimal burning

DOI: 10.1021/acs.est.6b04919
Environ. Sci. Technol. 2017, 51, 1423−1432

conditions produced a small amount of SOA (1.5 μg m^{-3}), while Heringa et al. did not observe SOA formation from pellet burner emissions during the stable burning phase.[44] They only measured appreciable SOA production from pellet burner emissions during the flaming phases.

The evolution of pellet boiler exhaust particle composition due to aging can be seen from the mass spectra from the beginning and the end of the "pellet-only" experiment (Figure 1, upper panel, Figure S3). The fraction of oxygenated hydrocarbon material (CHO) from total organics increased from 42% to 50%, while the fraction of hydrocarbons (CH) decreased from 53% to 48%. The upper panel of Figure 2 shows the temporal evolution of different OA species during the "pellet-only" experiment. The concentration of CHO material increased as the particles aged in the environmental chamber indicating particle oxidation during the experiments. The O:C ratio increased from 0.4 to 0.6, and the CHO family ion concentration increased from 1.1 μg m^{-3} to 1.6 μg m^{-3}. Concurrently, the CH concentration decreased from 2.9 μg m^{-3} to 2.5 μg m^{-3}. The O:C ratios were calculated using the updated method described by Canagaratna et al.[45]

The temporal evolution of different OA species (upper panel) and relative AMS composition (lower panel) is shown for a representative "mixed" experiment for comparison in Figure 3 (Experiment ID: HighP+α, Table 1). When α-pinene

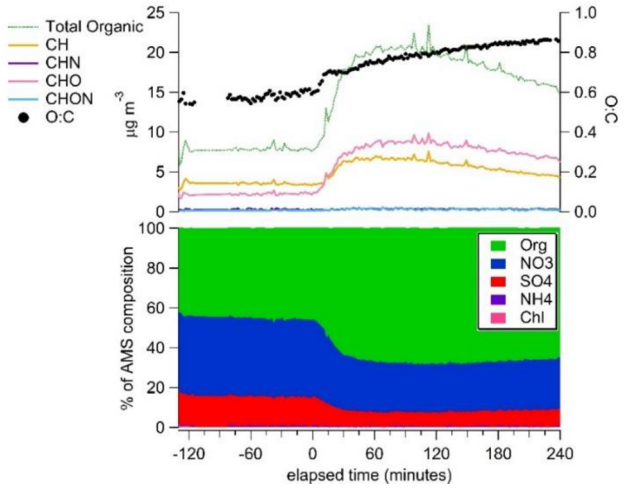

Figure 3. Temporal evolution of OA species (upper panel) and particle-phase species (lower panel) during the HighP+α experiment. At time 0 BL-lamps were turned on, and at time 240 the experiment was stopped. The feeding of pellet boiler exhaust is not shown.

was present in the environmental chamber, SOA formation occurred immediately after photochemistry was initiated. In contrast to the results from the "pellet-only" experiment, the organic fraction of the particles in this experiment increased by ~20% within 30 min of turning on the lights (Figure 3, lower panel). The additional organic mass in the particles is due to increased concentrations of hydrocarbon, CH, and oxygenated hydrocarbon species, CHO (Figure 3, upper panel). We assumed that the source of this additional organic material is primarily derived from α-pinene oxidation products. This assumption is justified by the fact that SOA mass produced by pellet boiler emissions in the absence of α-pinene was only 11.2% from the SOA mass produced during the analogous α-pinene experiment (HighAS+α experiment). In addition, the observed changes in the particle composition between the "pellet-only" and "mixed" experiments support this assumption. Figures 1 and S4 show that the relative abundance of CHO was substantially higher in the "mixed" experiments than it was in the "pellet-only" experiment, comprising 60% and 42% of total organics correspondingly. The relative abundance of CH was lower in the "mixed" experiments (36%) than the "pellet-only" experiment (53%). This all demonstrates that the organic material was more highly oxidized in the "mixed" experiment indicating a higher fraction of secondary organic material than in the primary organic material dominated "pellet-only" experiment.[46] Furthermore, the comparison of three mass spectra after aging from different experiments ("mixed", "α-pinene only", and "pellet-only") is shown in Figure 4. This figure indicates that the "mixed" experiment spectrum shares features with the other two: the "mixed" SOA spectrum can be best fitted by a combination of 75% "α-pinene only" SOA and 25% "pellet-only" SOA, with an unfitting residual of 22% of "mixed" SOA spectrum (for residual, see Figure S5). In addition, the CHON signal in the "mixed" spectrum (panel C) at m/z 43 is also observed in the "pellet-only" spectrum (panel A) but is absent from the "α-pinene only" spectrum (panel B). However, CHO at m/z 43 illustrates a distinct contribution from α-pinene: the "pellet-only" spectrum has very little CHO at m/z 43, but the "α-pinene only" and "mixed" spectra have a dominant contribution from CHO at m/z 43. These results support the conclusion that in the "mixed" experiment organic aerosol was composed of a combination organics both from pellet boiler exhaust and from the oxidation of α-pinene.

A more detailed look at the gas-phase chemistry that occurred during a typical "mixed" experiment is shown in Figure 5 (Experiment ID: HighP+α, Table 1). NO_x concentrations at the beginning of the experiment were 600 ppb (lower panel) highlighting that these are high-NO_x experiments, even after heavily diluting the pellet boiler emissions. Other experiments had similar NO_x levels with the exception of the single low-NO_x experiment that was performed for comparison. After the lights were turned on, photochemistry of NO_x and VOCs produced ~600 ppb ozone (lower panel). The α-pinene completely reacted within 30 min and generated typical oxidation products such as pinonaldehyde shown here as an example (upper panel). The total organic aerosol mass is shown again here to demonstrate that SOA generation occurred concurrently with α-pinene oxidation and pinonaldehyde formation. This is further evidence that in the "mixed" experiment most of the SOA mass is derived from α-pinene oxidation products and not from the pellet boiler emissions directly. Figure 5 also shows that SOA generation and pinonaldehyde formation occurred after NO was decreased close to 0 ppb due to suppression of hydroperoxide formation by NO.[17,25]

3.3. SOA Mass Yields. The SOA mass yields (Y) were calculated with eq 1

$$Y = \frac{\Delta M_0}{\Delta \mathrm{HC}} \quad (1)$$

where ΔM_0 is the maximum mass concentration of SOA formed (maximum OA mass−primary OA mass), and ΔHC is the mass concentration of α-pinene reacted.

Final SOA mass yields were corrected for particle wall losses, which varied from experiment to experiment. Particle wall losses were estimated for each experiment separately by calculating the aerosol mass loss rate constant according to Hao et al.[47] This method assumes first-order wall loss rate and

DOI: 10.1021/acs.est.6b04919
Environ. Sci. Technol. 2017, 51, 1423−1432

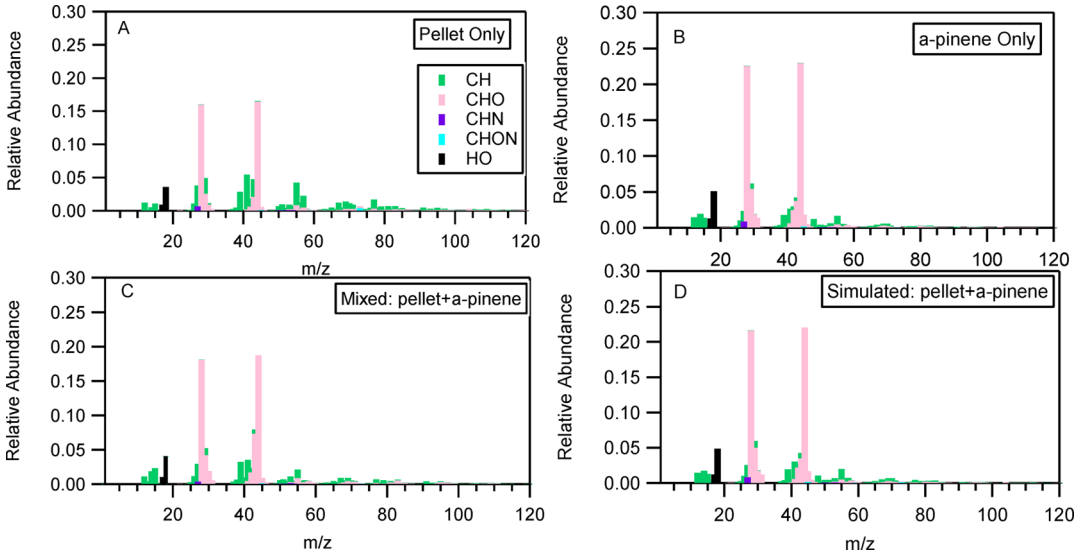

Figure 4. (A–C) The particle mass spectra of three different experiments and (D) the best simulated mass spectra of "mixed" SOA by a combination of 75% in mass from "α-pinene only" SOA and 25% from "pellet-only" SOA.

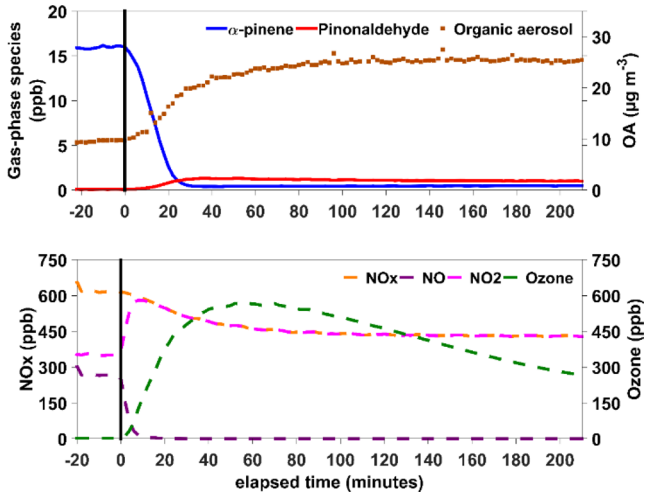

Figure 5. Temporal evolution of α-pinene, pinonaldehyde, and organic aerosol species (upper panel) and ozone and nitrogen oxides (lower panel) during the HighP+α experiment.

particle size independence. For the low-NO_x experiment the wall losses of aerosol particles were estimated using a particle size dependent wall loss correction.[48] The different wall loss corrections were applied in these two cases, because the low NO_x experiment conducted in the 10 m^3 chamber was not run for long enough to assume that no additional SOA was forming, hence the approach presented in Hao et al. was not applicable.

The left panel of Figure 6 summarizes the SOA mass yields for all experiments assuming α-pinene was the major SOA precursor. The experiment MedP+α3 was excluded from this analysis because the PTR-MS was under maintenance, and thus α-pinene concentrations could not be continuously monitored. OH exposures were calculated according to Barmet et al.[39]—explained in more detail in the SI. We can assume that OH chemistry dominated the oxidation chemistry inside the chamber (details from the SI). SOA mass yields from the high-NO_x experiments ranged from 11.0 to 19.4% (left panel of Figure 6). There is some variability in these values (which will be explained later), but all of them are substantially smaller than the maximum SOA mass yield observed during the low-NO_x experiment, which had an SOA mass yield of 34.1 ± 1.9%. The variation in organic mass loadings between all the experiments was small (Table 1), so the variation between yields in the high-NO_x experiments and the reduced SOA mass yield in the high-NO_x experiments cannot be explained by increased absorption due to differences in organic aerosol mass. Moreover, the concentration of α-pinene and OH exposures were similar in every experiment (Table 1), so neither of these can explain the differences in observed SOA mass yields either. Consequently, these results suggest that it was the high-NO_x concentrations emitted by the pellet boiler that reduced SOA formation from α-pinene. This conclusion is consistent with earlier studies conducted by Ng et al.[49] and Eddingsaas et al.[50] where they investigated SOA formation from α-pinene under both high- and low-NO_x conditions. Under high-NO_x conditions Ng et al.[49] measured SOA mass yields for α-pinene between 6.6%–15.8%, while Eddingsaas et al.[50] observed an SOA mass yield of 14.4%. Similar to results from this study, both groups measured higher SOA mass yields for α-pinene under low-NO_x conditions—37.9%–45.8% (Ng et al.[49]) and 25.7%–28.9% (Eddingsaas et al.[50]). Based on the results shown in the left panel of Figure 6 we can be confident that despite the use of two different approaches for wall loss correction the conclusions are valid. The difference in maximum yield between the low NO_x experiment and the analogous high NO_x experiment (LowP+α, Table 1) was greater than 300% (left panel of Figure 6)—a difference much larger than any uncertainty introduced from using two different approaches to the wall loss correction.

An alternative explanation for the reduced yields in the high-NO_x experiments is that the chemical properties of the primary particles emitted directly from the pellet boiler could have affected the SOA mass yields. In the "mixed" experiments the primary particle emissions effectively acted as a seed for the α-pinene SOA. Seed composition can influence SOA mass yields. For example, highly acidic seed increases SOA mass yields from α-pinene oxidation.[51,52] Recall from the methods that we investigated whether or not the primary particle emissions from the pellet boiler affected the SOA mass yields by conducting "α-pinene only" experiments using ammonium sulfate seed. Each

DOI: 10.1021/acs.est.6b04919
Environ. Sci. Technol. 2017, 51, 1423–1432

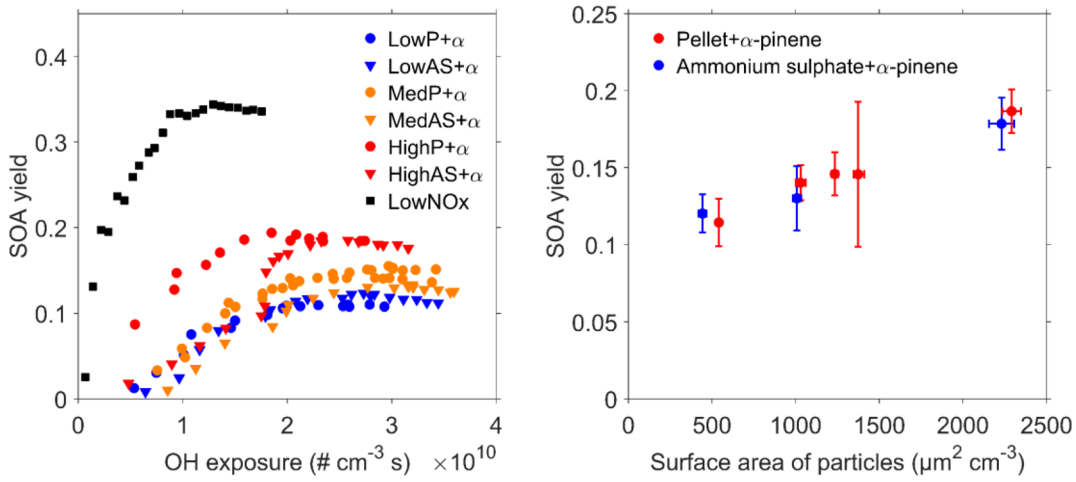

Figure 6. SOA yield as a function of OH exposure from high- and low-NO_x experiments (left panel). MedP+α stands for the experiments MedP+α1 and MedP+α2. The MedP+α3 experiment is missing, due to maintenance of PTR-MS during this experiment. SOA yield as a function of initial surface area of particles from high-NO_x experiments (right panel). Error bars for the *x*-axis are estimated from scatter in measurements of surface area of particles monitored by SMPS and for the *y*-axis from uncertainties in SP-AMS and PTR-MS measurements using square root of sum of squares of relative standard deviations (for the MedP+α3 experiment the yield error is estimated from uncertainties in SP-AMS and GC-MS measurements).

"mixed" SOA experiment has a matching "α-pinene only" experiment conducted with a similar mass of seed material, VOC-to-NO_x ratios and NO_x concentrations. The right panel of Figure 6 shows the SOA mass yields as a function of seed surface area for the two different types of seed used in these experiments—primary particles emitted by the pellet boiler ("pellet") and ammonium sulfate. When the initial surface area of particles was approximately the same, the observed yields were also similar regardless of the seed material.

It should be noted that recently, it has been shown that SOA yields can be underestimated due to wall losses of SOA-forming vapors during chamber experiments.[53−56] Wall deposition of vapors strongly affects SOA yields observed in the chamber. For this reason the yields reported here may be lower limits. Figure 6 also provides insight into the effect of vapor wall losses on yield and, further, on the reasons behind the variability in SOA yields observed between the high-NO_x experiments. For both types of seed the SOA mass yield increased with increasing initial seed surface area. It should be noted that similar clear correlation was not observed between the SOA yield and organic mass loading due to the small variability in the total organic masses. Figure 6 (right panel) illustrates that the observed yields were dependent on the condensation surface area of the seed particles used for each experiment. Furthermore, the seed surface area effect was similar for both types of seed used in these experiments. Hence, based on the right panel of Figure 6 it is clear that the material characteristics of primary particles emitted by the pellet boiler did not affect the mass yields, while the seed surface area available for the vapors, on the other hand, affected the yield due to competition for vapors between chamber wall surface and particle surface.

The results illustrate that pellet boiler exhaust reduced SOA yields from α-pinene. Moreover, our results demonstrate that the main factor contributing to decreased SOA mass yields in the presence of pellet boiler exhaust was elevated NO_x concentrations. The oxidation mechanisms, and thus oxidation products, of terpenes are different under high- versus low-NO_x conditions.[25,26,49] Elevated NO_x concentrations reduce RO_2 + RO_2 and RO_2 + HO_2 reactions while initiating RO_2 + NO reactions. This shift in reaction pathways of α-pinene produces organonitrate oxidation products with higher vapor pressures than oxidation products that are generated under the low-NO_x reaction pathways. Despite their higher vapor pressures, some organonitrate oxidation products will partition into the particle phase. This reaction pathway change was observed in "α-pinene only" experiments; under high-NO_x conditions the ratio of NO^+-to-NO_2^+ ions was 5.65 and verified our assumption that the nitrate existed in the chemical form of organonitrates (details from the SI and Figure S6).[42,57] In contrast, under low-NO_x conditions the ratio of NO^+-to-NO_2^+-ions was 2.5 suggesting the presence of ammonium nitrate. The formation of organonitrates was not observed in "mixed" experiments, since the mineral nitrates produced by the pellet boiler (see Results and Discussion section 3.1) interfered with the interpretation of the spectrum. However, we assume that also in "mixed" experiments the organonitrates were formed because we have shown that similar chemistry took place during "mixed" and "α-pinene only" experiments under high-NO_x conditions. Gas-phase organonitrate compounds were not detected in the gas-phase. This is likely because their concentrations were below the detection limit of the PTR-MS due to the low mixing ratios of α-pinene used in these experiments (14−20 ppb) to represent total monoterpene levels in hemiboreal forest environments.[58]

Anthropogenic-biogenic interactions in the atmosphere is an important, yet complex, topic. In this study, we used for the very first time a mixed system that combines the exhaust from a real anthropogenic emission source, the pellet boiler, and α-pinene as one example test system. Our results highlight the important influence of increased NO_x concentrations from anthropogenic sources on biogenic SOA formation processes. In this study system, the dominant effect of anthropogenic emissions on biogenic SOA formation was to reduce SOA mass yields by stimulating the high-NO_x oxidation pathway. This type of information is vital for understanding and simplifying model representations related to anthropogenic-biogenic interactions in the atmosphere. The pellet boilers can be considered as a model system for all continuously operated

DOI: 10.1021/acs.est.6b04919
Environ. Sci. Technol. 2017, 51, 1423−1432

wood-fired boilers,[59] hence we believe that the conclusion can be generalized to concern wood-fired boilers more generally. The NO_x effect would be different for different types of BVOCs because some terpenoids have increased SOA mass yields under high-NO_x conditions.[18] Future work should investigate the influence of other anthropogenic pollution sources on biogenic SOA formation to determine if the NO_x concentrations are the dominant factor affecting the SOA chemistry in other test systems. Furthermore, the ultimate anthropogenic effect on biogenic SOA formation is further complicated because primary particle emissions would likely increase SOA mass yields by providing additional organic aerosol mass thereby increasing background OA and increasing absorption. Future investigations should use regional modeling techniques to investigate the role of both increasing background OA and the influence of NO_x chemistry on biogenic SOA formation concurrently.

■ ASSOCIATED CONTENT

Supporting Information

The Supporting Information is available free of charge on the ACS Publications website at DOI: 10.1021/acs.est.6b04919.

Details about the cleaning procedure of the chamber prior to experiments and the instrumentation used in this study; description of the feeding procedure of the pellet boiler exhaust into the environmental chamber; detailed information about the experimental procedure for the low-NO_x experiment; detailed description about OH exposure calculation; arguments for the OH-chemistry dominance over ozonolysis; details about the formation and identification of organonitrate compounds; Table S1 (instrumentation used in this study); Table S2 (organic compounds calibrated for FTIR that were used to calculate THC values from the raw exhaust); Table S3 (maximum concentrations of formed ozone due to photochemistry during high-NO_x experiments); Figure S1 (schematic of the setup during the experiments conducted under high-NO_x conditions); Figure S2 (mass defect plot of the primary particulate composition of pellet boiler emission); Figure S3 (mass spectrum of organic aerosol composition from the end of the Pellet experiment); Figure S4 (mass spectrum of organic aerosol composition from the HighP+α experiment); Figure S5 (residuals for the best fitting between "mixed" and "simulated" cases); Figure S6 (NO and NO_2 ion signals from ammonium sulfate+α-pinene experiments conducted under high-NO_x and low-NO_x conditions); Figure S7 (schematic of the setup during the experiment conducted under low-NO_x conditions) (PDF)

■ AUTHOR INFORMATION

Corresponding Author

*Phone: +358-50-3164118. E-mail: annele.virtanen@uef.fi.

ORCID

Eetu Kari: 0000-0001-6611-7568

Pasi Yli-Pirilä: 0000-0002-7882-4574

Author Contributions

The manuscript was written through contributions of all authors. All authors have given approval to the final version of the manuscript.

Notes

The authors declare no competing financial interest.

■ ACKNOWLEDGMENTS

This work was financially supported by European Research Council (ERC Starting Grant 335478) and The Academy of Finland (grant no 272041 and 259005). The work of E. Kari was financially supported by University of Eastern Finland Doctoral Program in Environmental Physics, Health and Biology.

■ REFERENCES

(1) Atkinson, R. Atmospheric chemistry of VOCs and NOx. *Atmos. Environ.* **2000**, *34* (12−14), 2063−2101.

(2) Atkinson, R.; Arey, J. Atmospheric degradation of volatile organic compounds. *Chem. Rev.* **2003**, *103* (12), 4605−4638.

(3) Kanakidou, M.; Seinfeld, J. H.; Pandis, S. N.; Barnes, I.; Dentener, F. J.; Facchini, M. C.; Van Dingenen, R.; Ervens, B.; Nenes, A.; Nielsen, C. J.; et al. Organic aerosol and global climate modelling: a review. *Atmos. Chem. Phys.* **2005**, *5*, 1053−1123.

(4) Hallquist, M.; Wenger, J. C.; Baltensperger, U.; Rudich, Y.; Simpson, D.; Claeys, M.; Dommen, J.; Donahue, N. M.; George, C.; Goldstein, A. H.; et al. The formation, properties and impact of secondary organic aerosol: current and emerging issues. *Atmos. Chem. Phys.* **2009**, *9* (14), 5155−5236.

(5) Fehsenfeld, F.; Calvert, J. G.; Fall, R.; Goldan, P.; Guenther, A. B.; Hewitt, C. N.; Lamb, B.; Liu, S.; Trainer, M.; Westberg, H.; et al. Emissions of volatile organic compounds from vegetation and the implications for atmospheric chemistry. *Global Biogeochemical Cycles* **1992**, *6* (4), 389−430.

(6) Guenther, A.; Hewitt, C. N.; Erickson, D.; Fall, R.; Geron, C.; Graedel, T.; Harley, P.; Klinger, L.; Lerdau, M.; Mckay, W. A.; et al. A Global-Model of Natural Volatile Organic-Compound Emissions. *J. Geophys. Res.* **1995**, *100* (D5), 8873−8892.

(7) Goldstein, A. H.; Galbally, I. E. Known and unexplored organic constituents in the earth's atmosphere. *Environ. Sci. Technol.* **2007**, *41* (5), 1514−1521.

(8) Warneke, C.; McKeen, S. A.; de Gouw, J. A.; Goldan, P. D.; Kuster, W. C.; Holloway, J. S.; Williams, E. J.; Lerner, B. M.; Parrish, D. D.; Trainer, M. et al., Determination of urban volatile organic compound emission ratios and comparison with an emissions database. *J. Geophys. Res.* **2007**, *112*, (D10).10.1029/2006JD007930

(9) Apel, E. C.; Emmons, L. K.; Karl, T.; Flocke, F.; Hills, A. J.; Madronich, S.; Lee-Taylor, J.; Fried, A.; Weibring, P.; Walega, J.; et al. Chemical evolution of volatile organic compounds in the outflow of the Mexico City Metropolitan area. *Atmos. Chem. Phys.* **2010**, *10* (5), 2353−2375.

(10) Parrish, D. D.; Kuster, W. C.; Shao, M.; Yokouchi, Y.; Kondo, Y.; Goldan, P. D.; de Gouw, J. A.; Koike, M.; Shirai, T. Comparison of air pollutant emissions among mega-cities. *Atmos. Environ.* **2009**, *43* (40), 6435−6441.

(11) IPCC, *Climate Change 2013: The Physical Science Basis. Contribution of Working Group I to the Fifth Assessment Report of the Intergovernmental Panel on Climate Change*. Cambridge University Press: Cambridge, United Kingdom and New York, NY, USA, 2013; p 596.

(12) Shilling, J. E.; Zaveri, R. A.; Fast, J. D.; Kleinman, L.; Alexander, M. L.; Canagaratna, M. R.; Fortner, E.; Hubbe, J. M.; Jayne, J. T.; Sedlacek, A.; et al. Enhanced SOA formation from mixed anthropogenic and biogenic emissions during the CARES campaign. *Atmos. Chem. Phys.* **2013**, *13* (4), 2091−2113.

(13) Emanuelsson, E. U.; Hallquist, M.; Kristensen, K.; Glasius, M.; Bohn, B.; Fuchs, H.; Kammer, B.; Kiendler-Scharr, A.; Nehr, S.; Rubach, F.; et al. Formation of anthropogenic secondary organic aerosol (SOA) and its influence on biogenic SOA properties. *Atmos. Chem. Phys.* **2013**, *13* (5), 2837−2855.

(14) Carlton, A. G.; Pinder, R. W.; Bhave, P. V.; Pouliot, G. A. To What Extent Can. Biogenic SOA be Controlled? *Environ. Sci. Technol.* **2010**, *44* (9), 3376−3380.
(15) Hoyle, C. R.; Myhre, G.; Berntsen, T. K.; Isaksen, I. S. A. Anthropogenic influence on SOA and the resulting radiative forcing. *Atmos. Chem. Phys.* **2009**, *9* (8), 2715−2728.
(16) Goldstein, A. H.; Koven, C. D.; Heald, C. L.; Fung, I. Y. Biogenic carbon and anthropogenic pollutants combine to form a cooling haze over the southeastern United States. *Proc. Natl. Acad. Sci. U. S. A.* **2009**, *106* (22), 8835−8840.
(17) Kroll, J. H.; Ng, N. L.; Murphy, S. M.; Flagan, R. C.; Seinfeld, J. H. Secondary organic aerosol formation from isoprene photooxidation. *Environ. Sci. Technol.* **2006**, *40* (6), 1869−1877.
(18) Hoyle, C. R.; Boy, M.; Donahue, N. M.; Fry, J. L.; Glasius, M.; Guenther, A.; Hallar, A. G.; Hartz, K. H.; Petters, M. D.; Petaja, T.; et al. A review of the anthropogenic influence on biogenic secondary organic aerosol. *Atmos. Chem. Phys.* **2011**, *11* (1), 321−343.
(19) Odum, J. R.; Hoffmann, T.; Bowman, F.; Collins, D.; Flagan, R. C.; Seinfeld, J. H. Gas/particle partitioning and secondary organic aerosol yields. *Environ. Sci. Technol.* **1996**, *30* (8), 2580−2585.
(20) Pankow, J. F. An Absorption-Model of Gas-Particle Partitioning of Organic-Compounds in the Atmosphere. *Atmos. Environ.* **1994**, *28* (2), 185−188.
(21) Asa-Awuku, A.; Miracolo, M. A.; Kroll, J. H.; Robinson, A. L.; Donahue, N. M. Mixing and phase partitioning of primary and secondary organic aerosols. *Geophys. Res. Lett.* **2009**, *36*, L15827.
(22) Jang, M. S.; Czoschke, N. M.; Lee, S.; Kamens, R. M. Heterogeneous atmospheric aerosol production by acid-catalyzed particle-phase reactions. *Science* **2002**, *298* (5594), 814−817.
(23) Jang, M.; Czoschke, N. M.; Northcross, A. L. Atmospheric organic aerosol production by heterogeneous acid-catalyzed reactions. *ChemPhysChem* **2004**, *5* (11), 1646−1661.
(24) Jang, M. S.; Kamens, R. M. Atmospheric secondary aerosol formation by heterogeneous reactions of aldehydes in the presence of a sulfuric acid aerosol catalyst. *Environ. Sci. Technol.* **2001**, *35* (24), 4758−4766.
(25) Presto, A. A.; Hartz, K. E. H.; Donahue, N. M. Secondary organic aerosol production from terpene ozonolysis. 2. Effect of NOx concentration. *Environ. Sci. Technol.* **2005**, *39* (18), 7046−7054.
(26) Lim, Y. B.; Ziemann, P. J. Products and mechanism of secondary organic aerosol formation from reactions of n-alkanes with OH radicals in the presence of NOx. *Environ. Sci. Technol.* **2005**, *39* (23), 9229−9236.
(27) Hoffmann, T.; Odum, J. R.; Bowman, F.; Collins, D.; Klockow, D.; Flagan, R. C.; Seinfeld, J. H. Formation of organic aerosols from the oxidation of biogenic hydrocarbons. *J. Atmos. Chem.* **1997**, *26* (2), 189−222.
(28) Kulmala, M.; Vehkamaki, H.; Petaja, T.; Dal Maso, M.; Lauri, A.; Kerminen, V. M.; Birmili, W.; McMurry, P. H. Formation and growth rates of ultrafine atmospheric particles: a review of observations. *J. Aerosol Sci.* **2004**, *35* (2), 143−176.
(29) Toscano, G.; Riva, G.; Pedretti, E. F.; Corinaldesi, F.; Mengarelli, C.; Duca, D. Investigation on wood pellet quality and relationship between ash content and the most important chemical elements. *Biomass Bioenergy* **2013**, *56*, 317−322.
(30) Stelte, W.; Holm, J. K.; Sanadi, A. R.; Barsberg, S.; Ahrenfeldt, J.; Henriksen, U. B. A study of bonding and failure mechanisms in fuel pellets from different biomass resources. *Biomass Bioenergy* **2011**, *35* (2), 910−918.
(31) Johansson, L. S.; Leckner, B.; Gustavsson, L.; Cooper, D.; Tullin, C.; Potter, A. Emission characteristics of modern and old-type residential boilers fired with wood logs and wood pellets. *Atmos. Environ.* **2004**, *38* (25), 4183−4195.
(32) Sippula, O.; Hytonen, K.; Tissari, J.; Raunemaa, T.; Jokiniemi, J. Effect of wood fuel on the emissions from a top-feed pellet stove. *Energy Fuels* **2007**, *21* (2), 1151−1160.
(33) Boman, C.; Pettersson, E.; Westerholm, R.; Bostrom, D.; Nordin, A. Stove Performance and Emission Characteristics in Residential Wood Log and Pellet Combustion, Part 1: Pellet Stoves. *Energy Fuels* **2011**, *25*, 307−314.
(34) Riva, G.; Pedretti, E. F.; Toscano, G.; Duca, D.; Pizzi, A. Determination of polycyclic aromatic hydrocarbons in domestic pellet stove emissions. *Biomass Bioenergy* **2011**, *35* (10), 4261−4267.
(35) Leskinen, A.; Yli-Pirila, P.; Kuuspalo, K.; Sippula, O.; Jalava, P.; Hirvonen, M. R.; Jokiniemi, J.; Virtanen, A.; Komppula, M.; Lehtinen, K. E. J. Characterization and testing of a new environmental chamber. *Atmos. Meas. Tech.* **2015**, *8* (6), 2267−2278.
(36) Lamberg, H.; Sippula, O.; Tissari, J.; Jokiniemi, J. Effects of Air Staging and Load on Fine-Particle and Gaseous Emissions from a Small-Scale Pellet Boiler. *Energy Fuels* **2011**, *25* (11), 4952−4960.
(37) Chirico, R.; DeCarlo, P. F.; Heringa, M. F.; Tritscher, T.; Richter, R.; Prevot, A. S. H.; Dommen, J.; Weingartner, E.; Wehrle, G.; Gysel, M.; et al. Impact of aftertreatment devices on primary emissions and secondary organic aerosol formation potential from in-use diesel vehicles: results from smog chamber experiments. *Atmos. Chem. Phys.* **2010**, *10* (23), 11545−11563.
(38) Wildt, J.; Mentel, T. F.; Kiendler-Scharr, A.; Hoffmann, T.; Andres, S.; Ehn, M.; Kleist, E.; Musgen, P.; Rohrer, F.; Rudich, Y.; et al. Suppression of new particle formation from monoterpene oxidation by NOx. *Atmos. Chem. Phys.* **2014**, *14* (6), 2789−2804.
(39) Barmet, P.; Dommen, J.; DeCarlo, P. F.; Tritscher, T.; Praplan, A. P.; Platt, S. M.; Prevot, A. S. H.; Donahue, N. M.; Baltensperger, U. OH clock determination by proton transfer reaction mass spectrometry at an environmental chamber. *Atmos. Meas. Tech.* **2012**, *5* (3), 647−656.
(40) Platt, S. M.; El Haddad, I.; Zardini, A. A.; Clairotte, M.; Astorga, C.; Wolf, R.; Slowik, J. G.; Temime-Roussel, B.; Marchand, N.; Jezek, I.; et al. Secondary organic aerosol formation from gasoline vehicle emissions in a new mobile environmental reaction chamber. *Atmos. Chem. Phys.* **2013**, *13* (18), 9141−9158.
(41) Heringa, M. F.; DeCarlo, P. F.; Chirico, R.; Lauber, A.; Doberer, A.; Good, J.; Nussbaumer, T.; Keller, A.; Burtscher, H.; Richard, A.; et al. Time-Resolved Characterization of Primary Emissions from Residential Wood Combustion Appliances. *Environ. Sci. Technol.* **2012**, *46* (20), 11418−11425.
(42) Alfarra, M. R.; Paulsen, D.; Gysel, M.; Garforth, A. A.; Dommen, J.; Prevot, A. S. H.; Worsnop, D. R.; Baltensperger, U.; Coe, H. A mass spectrometric study of secondary organic aerosols formed from the photooxidation of anthropogenic and biogenic precursors in a reaction chamber. *Atmos. Chem. Phys.* **2006**, *6*, 5279−5293.
(43) Rollins, A. W.; Fry, J. L.; Hunter, J. F.; Kroll, J. H.; Worsnop, D. R.; Singaram, S. W.; Cohen, R. C. Elemental analysis of aerosol organic nitrates with electron ionization high-resolution mass spectrometry. *Atmos. Meas. Tech.* **2010**, *3* (1), 301−310.
(44) Heringa, M. F.; DeCarlo, P. F.; Chirico, R.; Tritscher, T.; Dommen, J.; Weingartner, E.; Richter, R.; Wehrle, G.; Prevot, A. S. H.; Baltensperger, U. Investigations of primary and secondary particulate matter of different wood combustion appliances with a high-resolution time-of-flight aerosol mass spectrometer. *Atmos. Chem. Phys.* **2011**, *11* (12), 5945−5957.
(45) Canagaratna, M. R.; Jimenez, J. L.; Kroll, J. H.; Chen, Q.; Kessler, S. H.; Massoli, P.; Ruiz, L. H.; Fortner, E.; Williams, L. R.; Wilson, K. R.; et al. Elemental ratio measurements of organic compounds using aerosol mass spectrometry: characterization, improved calibration, and implications. *Atmos. Chem. Phys.* **2015**, *15* (1), 253−272.
(46) Jimenez, J. L.; Canagaratna, M. R.; Donahue, N. M.; Prevot, A. S. H.; Zhang, Q.; Kroll, J. H.; DeCarlo, P. F.; Allan, J. D.; Coe, H.; Ng, N. L.; et al. Evolution of Organic Aerosols in the Atmosphere. *Science* **2009**, *326* (5959), 1525−1529.
(47) Hao, L. Q.; Romakkaniemi, S.; Yli-Pirila, P.; Joutsensaari, J.; Kortelainen, A.; Kroll, J. H.; Miettinen, P.; Vaattovaara, P.; Tiitta, P.; Jaatinen, A.; et al. Mass yields of secondary organic aerosols from the oxidation of alpha-pinene and real plant emissions. *Atmos. Chem. Phys.* **2011**, *11* (4), 1367−1378.

DOI: 10.1021/acs.est.6b04919
Environ. Sci. Technol. 2017, 51, 1423−1432

(48) Mcmurry, P. H.; Grosjean, D. Gas and Aerosol Wall Losses in Teflon Film Smog Chambers. *Environ. Sci. Technol.* **1985**, *19* (12), 1176−1182.
(49) Ng, N. L.; Chhabra, P. S.; Chan, A. W. H.; Surratt, J. D.; Kroll, J. H.; Kwan, A. J.; McCabe, D. C.; Wennberg, P. O.; Sorooshian, A.; Murphy, S. M.; et al. Effect of NOx level on secondary organic aerosol (SOA) formation from the photooxidation of terpenes. *Atmos. Chem. Phys.* **2007**, *7* (19), 5159−5174.
(50) Eddingsaas, N. C.; Loza, C. L.; Yee, L. D.; Chan, M.; Schilling, K. A.; Chhabra, P. S.; Seinfeld, J. H.; Wennberg, P. O. alpha-pinene photooxidation under controlled chemical conditions - Part 2: SOA yield and composition in low- and high-NOx environments. *Atmos. Chem. Phys.* **2012**, *12* (16), 7413−7427.
(51) Czoschke, N. M.; Jang, M.; Kamens, R. M. Effect of acidic seed on biogenic secondary organic aerosol growth. *Atmos. Environ.* **2003**, *37* (30), 4287−4299.
(52) Czoschke, N. M.; Jang, M. S. Acidity effects on the formation of alpha-pinene ozone SOA in the presence of inorganic seed. *Atmos. Environ.* **2006**, *40* (23), 4370−4380.
(53) Zhang, X.; Cappa, C. D.; Jathar, S. H.; Mcvay, R. C.; Ensberg, J. J.; Kleeman, M. J.; Seinfeld, J. H. Influence of vapor wall loss in laboratory chambers on yields of secondary organic aerosol. *Proc. Natl. Acad. Sci. U. S. A.* **2014**, *111* (16), 5802−5807.
(54) Zhang, X.; Schwantes, R. H.; McVay, R. C.; Lignell, H.; Coggon, M. M.; Flagan, R. C.; Seinfeld, J. H. Vapor wall deposition in Teflon chambers. *Atmos. Chem. Phys.* **2015**, *15* (8), 4197−4214.
(55) Yeh, G. K.; Ziemann, P. J. Gas-Wall Partitioning of Oxygenated Organic Compounds: Measurements, Structure-Activity Relationships, and Correlation with Gas Chromatographic Retention Factor. *Aerosol Sci. Technol.* **2015**, *49* (9), 727−738.
(56) Kokkola, H.; Yli-Pirila, P.; Vesterinen, M.; Korhonen, H.; Keskinen, H.; Romakkaniemi, S.; Hao, L.; Kortelainen, A.; Joutsensaari, J.; Worsnop, D. R.; et al. The role of low volatile organics on secondary organic aerosol formation. *Atmos. Chem. Phys.* **2014**, *14* (3), 1689−1700.
(57) Farmer, D. K.; Matsunaga, A.; Docherty, K. S.; Surratt, J. D.; Seinfeld, J. H.; Ziemann, P. J.; Jimenez, J. L. Response of an aerosol mass spectrometer to organonitrates and organosulfates and implications for atmospheric chemistry. *Proc. Natl. Acad. Sci. U. S. A.* **2010**, *107* (15), 6670−6675.
(58) Noe, S. M.; Huve, K.; Niinemets, u.; Copolovici, L. Seasonal variation in vertical volatile compounds air concentrations within a remote hemiboreal mixed forest. *Atmos. Chem. Phys.* **2012**, *12* (9), 3909−3926.
(59) Lillieblad, L.; Szpila, A.; Strand, M.; Pagels, J.; Rupar-Gadd, K.; Gudmundsson, A.; Swietlicki, E.; Bohgard, M.; Sanati, M. Boiler operation influence on the emissions of submicrometer-sized particles and polycyclic aromatic hydrocarbons from biomass-fired grate boilers. *Energy Fuels* **2004**, *18* (2), 410−417.

DOI: 10.1021/acs.est.6b04919
Environ. Sci. Technol. 2017, 51, 1423−1432